Aircraft Strain WSN Powered by Heat Storage Harvesting

L. V. Allmen, G. Bailleul, Th. Becker, J.-D. Decotignie, *Fellow, IEEE*, M. E. Kiziroglou, *Senior Member, IEEE*, C. Leroux, P. D. Mitcheson, *Senior Member, IEEE*, J. Müller, D. Piguet, T. T. Toh, A. Weisser, S. W. Wright, and E. M. Yeatman, *Fellow, IEEE*

***Abstract*—The combination of ultra-low-power wireless communications and energy harvesting enables the realization of autonomous wireless sensor networks. Such networks can be usefully applied in commercial aircraft where wireless sensing solutions contribute to weight reduction and increased ease of installation and maintenance. This paper presents, for the first time, a complete energy-autonomous wireless strain monitoring system for aircraft. The system is based on a multimode wireless time-division multiple access (TDMA) medium access control (MAC) protocol that supports automatic configuration and a time-stamping accuracy better than 1 ms. The energy supply depends solely on an innovative thermoelectric energy harvester, which takes advantage of the changes in environmental temperature during takeoff and landing. The system was successfully integrated and passed the functional and flight-clearance tests that qualify it for use in a flight-test installation.**

***Index Terms*—Aircraft, energy harvesting, heat storage, sensor, strain, thermoelectric, wireless sensor networks (WSNs).**

I. Introduction

THIS paper presents a wireless, energy-autonomous strain monitoring system for aircraft applications. The system aims to provide aircraft operators with a new tool for the predictive maintenance of airframes, with minimal weight impact and low usage costs. The main benefit is a significant reduction of maintenance costs by allowing part replacement based on stress measurement and analysis, instead of the automatic substitution of elements that have gone through their quota of flight cycles or hours. The minimal weight impact stems from reduced cabling due to the wireless nature of the system. The usage and maintenance costs are low due to the combination of energy harvesting and ultra-low-power communications, as this eliminates the need for batteries, which would require regular replacement.

In order to enhance relevance and applicability to real industrial requirements, the wireless strain monitoring network presented here was developed in response to industrial requirements expressed by an aircraft manufacturer for two use cases. The first addresses load monitoring on the vertical tail plane (VTP) of commercial aircraft. Measurements sessions are triggered by the aircraft avionics when a flight sequence that may involve heavy loads on the VTP is detected from the observation of other flight parameters. Up to ten measurements sessions of 30 s each per flight are expected. The second regards the monitoring of strain in the landing gear. In this case, measurements are acquired continuously between landing gear extension and until the aircraft has reached a low speed on the ground. The specified maximal data acquisition duration is 500 s. For both cases, the required measurement sampling rates are between 120 and 500 Hz. All data samples have to be time-stamped with synchronization error up to 1 ms, in order to correlate with data produced by other systems. The system has been fully implemented in hardware and successfully underwent functional and qualification tests, showing sustainability to heavy vibrations and extreme temperatures (+85 to −55 °C) while respecting a challenging maximal electromagnetic field emissions constraint (DO-160 Cat. H Curve C1 [1]).

The innovation in implementing this monitoring system lies in the development of a low-power networking protocol, with duty-cycled sensor operation scheduling. This allows strain measurements at specific time intervals, with adequate sampling rates, within a given energy budget. In addition, a dynamic thermoelectric harvester was developed, with new insulating and power management techniques that lead to significant performance advancement in comparison with the current state of the art. Furthermore, a system-level codesign approach was adopted, providing an integrated system with commensurate energy demand and supply, and system-level packaging that meets the specific physical, vibration and electromagnetic specifications required for aircrafts.

Manuscript received September 6, 2016; revised December 3, 2016; accepted December 9, 2016. Date of publication January 16, 2017; date of current version August 9, 2017. This work was supported by the Clean Sky Joint Technology Initiative under Grant JTI-CS-2010-1-SFWA-01-016.

L. V. Allmen, J.-D. Decotignie, and D. Piguet are with the CSEM, 2002 Neuchatel, Switzerland.

G. Bailleul and C. Leroux are with Serma Ingenierie 31700 Cornebarrieu, France.

T. Becker is with Airbus Group Innovations, 81663 Munich, Germany.

M. E. Kiziroglou, P. D. Mitcheson, T. T. Toh, S. W. Wright, and E. M. Yeatman are with Imperial College London, London, SW7 2BT, U.K. (e-mail: m.kiziroglou@imperial.ac.uk).

J. Muller and A. Weisser are with Airbus Operation GmbH, Am Kreetslag, 21111 Hamburg, Germany.

Color versions of one or more of the figures in this paper are available online at http://ieeexplore.ieee.org.

Digital Object Identifier 10.1109/TIE.2017.2652375

II. Related Work

A. Wireless Sensors in Aircraft

Research on wireless communications for aircraft monitoring and control has seen growing interest in the last decade. This is due to anticipated cabling reduction and maintenance benefits, as well as to the increasing availability of the underlying technologies (low-power electronics, protocols, and energy harvesting). In [2], various aircraft applications of wireless sensors and actuators are discussed. Systems that are likely to become available in the short term include cabin control (environment, seat occupancy, seatbelts [3]), tire pressure monitoring [4], structural health monitoring [5], and even in-flight entertainment [6]. For such applications, the approach developed in this paper is based on an energy-autonomous sensor node (SN) powered by a thermoelectric energy harvester and operating with a low-power communication protocol that allows optimized duty-cycling operation.

B. Protocols for Wireless Sensor Networks

In wireless communications, the main desirable features are robustness, lifetime, low energy, temporal guarantees (i.e., time awareness) and ease of deployment and maintenance. These features can generally be provided by the medium access control (MAC) protocol layer, routing and transport, discovery and network management, and an application layer for easy use.

In local area wireless sensor network (WSN) applications, routing through individual SNs is often not necessary because a central wireless data concentrator (WDC) based topology can be adopted and single hop links are sufficient. In addition, a transport layer is not required as typically the system has to support only two types of traffic: measurement transmissions and control commands. Buffering, retransmissions, and permanent recording are provided by the application layer. A feature of special interest is synchronization, because measurements must be related in time. A brief overview of the context in which the MAC protocol architecture introduced in this paper was developed is presented later.

The main difference between the requirements of a WSN MAC and those of wireless local area networks is in the balance between energy efficiency and throughput capacity. Energy efficiency is usually a priority for WSNs. This is typically achieved through duty cycling, at the cost of an increased transmission delay and a lower maximum throughput. In addition, a WSN MAC must minimize idle listening (the time spent listening to an empty channel), overhearing (the time spent listening to traffic addressed to other nodes), overemitting (sending messages when the destination node is saving energy in sleep mode), collisions, and its own overhead (headers and MAC-level signaling).

Research on MAC protocols designed specifically for WSNs started toward the end of the 90s, and it has been receiving a lot of attention from the research community since the beginning of the current decade. According to Langendoen and Meier [7], MAC protocols for WSNs may be categorized into random access, slotted, frame-based, and hybrid protocols.

In random access, nodes contend for the medium with the risk of collisions. WiseMAC [8] is an ultra-low-power contention MAC that uses preamble sampling and pairwise exchange of schedules to reach close to ideal performances in medium to low traffic [7]. Slotted MACs establish a common sense of time through synchronization. Once synchronized, operation is distributed along a sequence of activity and sleep cycles. During the active part, nodes exchange information using contention access. Protocols differ in the way they end or adapt the size of activity. S-MAC has a fixed duration, thus limiting the maximum traffic to the duty cycle between the active part and the cycle time, whereas T-MAC adapts size to traffic. IEEE 802.15.4 in its beacon-oriented version [without guaranteed time slot (GTS)] is another example of this protocol type. They all have the drawback of grouping all the exchanges at the beginning of the cycle, thus increasing the probability of collision and limiting the traffic. To achieve low latency, the cycle must be small, leading to high power consumption.

Frame-based protocols allow slot grouping into frames and control medium access by scheduled assignment of nodes to slots, thereby eliminating contention [7]. They are called time-division multiple access (TDMA) or pure-TDMA protocols. In general, schedules are difficult to establish, especially in the presence of moving nodes or fluctuating link quality. In particular, handling retries due to transmission errors leads either to complex schemes or large inefficiency (e.g., systematic reservation of a retry slot for each transmission slot). TDMA-based solutions are very efficient in cases of high and constant loads. Low but still constant load may also be handled efficiently by compensating clock drift as in [9]. Solutions have been designed to manage efficiently variable loads at the expense of higher complexity [10]. An additional drawback of TDMA-based protocols is the need for coordination when different networks are installed in the same area, to avoid collisions. Some solutions like Bluetooth or WirelessHART adopt a mixed TDMA/FDMA scheme in which the successive transmissions are done on different channels. Minimizing energy consumption by scheduling has been investigated in [11]–[15]. The basic idea is to schedule nodes to operate only during an assigned time slot and otherwise be at sleep mode. Hybrid protocols such as Crankshaft [16] combine TDMA with CSMA to reduce collision probability and improve efficiency in the presence of low or variable traffic.

WirelessHART, ISA 100.11a, and WIA-PA are three IEC standards for industrial wireless communication at the sensor level. They are based on IEEE 802.15.4e, the real-time extension of IEEE 802.15.4 [17]. This standard defines three interesting options, low latency determinist networks (LLDN) for factory automation, time-slotted channel hopping (TSCH) for process automation, and deterministic and synchronous multichannel extension (DSME). All three are pure-TDMA protocols. They are based on an extension of the GTS principles, which removes the limits of GTS in terms on number of slots. The beacon format is also enhanced with additional information. The slot assignment is negotiated during the association process, but it may be changed at runtime via further negotiations. In other words, slot assignments may change but not rapidly; in particular, it is not possible to change this assignment from one beacon interval to the next.

On clock synchronization, several articles propose WSN solutions with low complexity and energy efficiency in mind. Among popular solutions are RBS [18], network-wide time synchronization protocol [19], flooding time synchronization protocol [20], and scalable lightweight time sync protocol [21]. These options have been assessed against the typical requirements of local WSN applications and the TDMA protocol type is chosen for the development of a MAC protocol specifically for local single-hop, synchronized data acquisition. This choice is suitable for industrial environments where deterministic communications are preferable. The architecture of the proposed protocol is presented in Section IV, along with a detailed description and evaluation of the implementation used in this paper.

C. Energy Harvesting for Aircraft Sensors

A variety of harvesting-powered WSNs have been proposed [22]. Aircraft specific studies on piezoelectric vibration harvesting highlight the importance of broadband operation and employ techniques such as bimorph stops [23]. Large-scale piezoelectric devices have been used to power aircraft SNs for structural monitoring [24]. The effectiveness of piezoelectric harvesting for unmanned aerial vehicles has been also studied in comparison with solar solutions, showing power outputs of 13 μW/cm^3 and 41 mW/cm^2, respectively [25], [26]. However, the applicability of solar harvesting is limited because direct light is not available in typical internal sensor locations. On the other hand, state-of-the-art indoor lighting power lies in the $1-10\,\mu$W/cm^2 range.

While piezoelectric device implementations with higher power exist and have been proposed for aircraft SNs (e.g., 240 μW/cm^3 at 67 Hz, 0.4 g [27]), resonant operation requirements have prevented their use. Solutions such nonlinear piezoelectric and hybrid piezoelectric/inductive devices, as well as new piezoelectric materials have been studied for aircraft SNs using simulation [28]. However, implementations with the required power density have not yet been reported.

The potential of RF power delivery for aircraft sensors has also been explored, showing critical efficiency dependence on wave incident angle [29]. Experimental results demonstrate delivered power of 200 μW at 1 m distance, and strain measurements from an RF-powered strain sensor [30].

The applicability of TEG harvesting in aircraft WSNs depends on the availability of temperature gradient in the close vicinity of the desirable sensor locations, with good thermal contacts to both a hot body and a cold body. To address these limitations, a recently developed dynamic TEG harvesting approach [31], [32] is adopted in this paper.

III. Architecture

A. Network Architecture

In the proposed multicell WSN topology, the cells are linked to a central server through a wired network (Ethernet). Each cell consists of a WDC and up to 20 SNs. This sensor population number was chosen in order to potentially allow deployment over a large fuselage surface (e.g., up to 10 m^2) such as the aircraft VTP for the first use case defined in Section I or on the various different locations of interest of an aircraft landing gear for the second use case. The expected SN to WDC distance is in the range of 10–20 m, allowing transmission operations at 0 dBm with sufficient link margin. The WDC tasks are cell configuration (SN discovery), TDMA control (SN slot assignment), the relaying of commands and data between the server and the SNs, and the synchronization of the cell with the server time. The WDC is connected to the aircraft power supply, thus it does not require low-power operation. In contrast, SNs must be energy autonomous. Their task is to perform and transmit strain measurements on request by the server. This architecture is shown in Fig. 1. A cell may have an optional extra WDC to improve robustness. The SN and WDC platforms have many common parts, reducing development costs. The SN has an analog-to-digital (ADC) circuit to acquire measurements, while the WDC has an Ethernet interface to the WSN server.

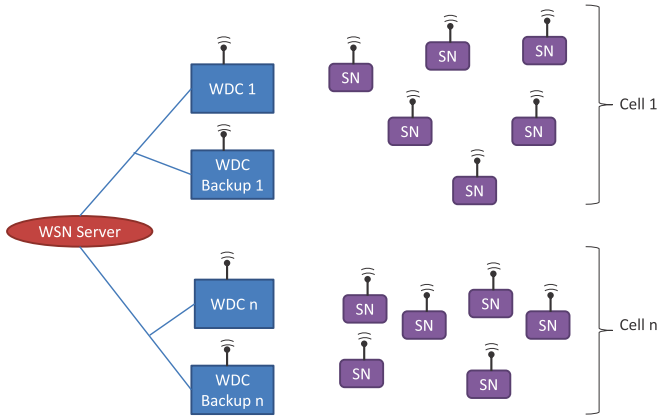

Fig. 1. Network architecture.

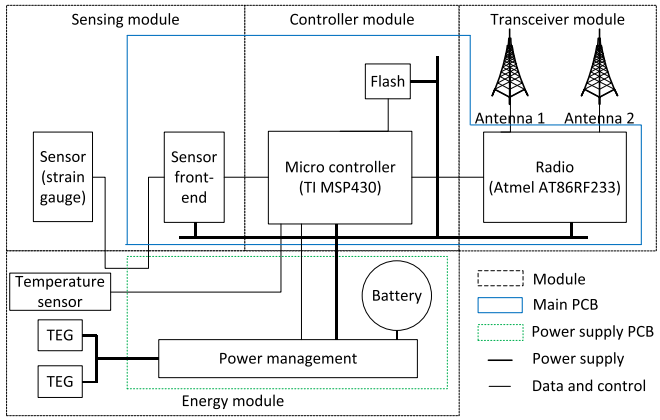

Fig. 2. SN architecture.

B. Sensor Node

A block diagram of the SN is shown in Fig. 2. The wireless interface is an Atmel AT86RF231/233. It supports antenna diversity for better reliability. The system is controlled by a Texas Instruments MSP430F5437A MCU. Among its advantages are

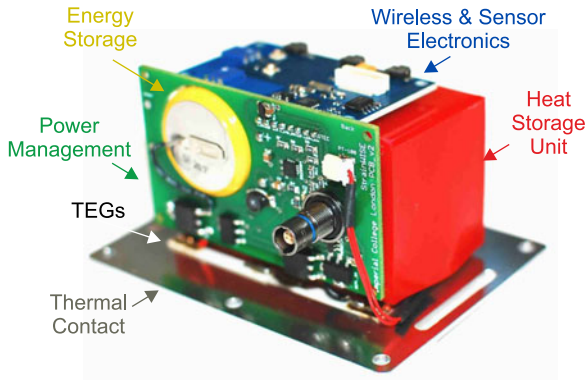

Fig. 3. Assembled SN (unpackaged).

TABLE I
COMPARISON WITH OTHER KNOWN TDMA PROTOCOLS

Feature	802. 15.4	LLDN	DSME	TSCH	LMAC	This Paper
Join complexity	High	High	High	High	Low	Low
Independent scheduling	Part	Part	Part	No	No	Full
Efficient acknowledgment	No[a]	Yes	No[a]	No[a]	No[a]	Yes
Operation modes	Ext	Ext	Ext	Ext	Ext	Int
Dynamic slot assignment	No	Retries	No	No	No	Yes
Adaptive no. of repetitions	No	[b]	No	No	No	Yes
Beacon diversity	No	No	No	No	NA	Yes

[a]Immediate
[b]Possible

numerous serial interfaces (UART/SPI/I2C), large RAM and program memory space, as well as low-power consumption in operation and an ultra-low-power sleep mode. The MCU controls the measurement acquisition performed by a Semtech SX8724S ADC, which is connected to the strain sensor (Wheatstone bridge strain gauge), again chosen for its low current consumption, especially in sleep mode. A 1-MB low-power flash memory has been added to allow the recording of all measurements taken during a typical flight in case the wireless communication fails. Sensing, controller, and transceiver parts are on the same PCB, while the power supply electronics are put on a second board. This distribution is optimal in terms of size, flexibility, and project management. A photograph of the (unpackaged) assembled SN is given in Fig. 3. The total size and weight of the unpackaged SN are 64 × 38 × 40 mm and 141 g, respectively.

The WDC shares the controller and transceiver modules with the SNs, but it doesn't carry an ADC, as it doesn't acquire measurements. It is directly connected to the WSN server via a Lantronix XPort connector, chosen to fit specific size and environmental constraints. It is powered directly by the aircraft power supply network.

IV. WIRELESS COMMUNICATION

The communication system is designed for up to 1 kB/s useful data rate per node (2 bytes per sample at 500 Hz) during acquisition and up to 20 nodes per cell. The nodes must be synchronized with the server to allow time stamping of each data sample. Power consumption must be minimal to ensure that SNs operate within an energy budget. Phases when the aircraft is nonoperational are critical because then no power can be harvested. Due to the propagation environment (metallic obstacles in particular), link quality fluctuation may occur. Finally, the wireless protocol must support an installation procedure with minimum human intervention.

A. Protocol Architecture

In this section, a centrally controlled TDMA protocol for low-power applications is introduced. Like IEEE 802.15.4e, most TDMA protocols assume a fixed traffic, at least for some duration, and do not allow fast dynamic runtime adaptations. This leads to oversubscription of slots at maximum traffic and waste of energy when the traffic is lower. In addition, it is not easy to implement operation modes with highly different traffic patterns. Similarly, most protocols reserve slots for retransmissions in a fixed manner. In practice though, only a few links experience errors, leading to inefficient management of available slots. To address this, a dynamic assignment of retransmission slots is adopted, similar to the LLDN protocol.

Using relays can improve reliability at the expense of latency [33]. Following this idea, we employ here a redundant WDC to increase reliability without sacrificing latency. The redundant WDC transmits a copy of the beacon just after the primary WDC, listens to the transmission of each SN, and forwards the result to wired network. This scheme increases reliability where it is most important (beacon reception) at the expense of a slight power increase (a given SN will only listen to the redundant beacon if it did not get the primary one).

Several known TDMA protocols are compared in Table I. LMAC [7] has been included for reference as a low-power TDMA protocol. The different criteria are joining complexity, scheduling dependence to the MAC protocol, efficiency of acknowledgment, capability of setting global operation modes, dynamic slot assignment, adaptable number of retransmission attempts, and beacon diversity. The join procedure complexity is quite high for the 802.15.4 family, which also does not feature dynamic slot assignment from one beacon to the next.

The acknowledgment process is more energy efficient both for LLDN and the proposed protocol, as it is implemented globally in the beacons, whereas it is immediate and per packet in the other proposals. In addition, LLDN and the proposed protocol can improve reliability for the same bandwidth use while reducing power consumption and latency, by dynamic bandwidth allocation for retransmission attempts on a link-by-link basis. The other protocols allocate fixed bandwidth for retries independently of the link quality, which may be overprovisioning for good links and insufficient for bad links.

The proposed protocol also implements global modes of operations to support advanced SN sleep mode management. This is an important unique feature, as in other solutions such modes must be implemented externally to the protocol, introducing significant traffic and power overhead. Finally, the proposed protocol allows beacon diversity to improve

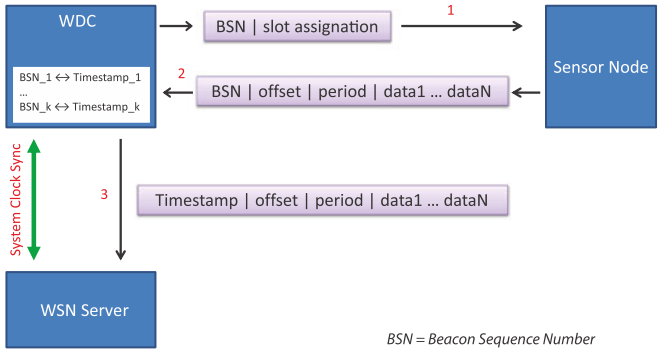

Fig. 4. Wireless synchronization for time stamping.

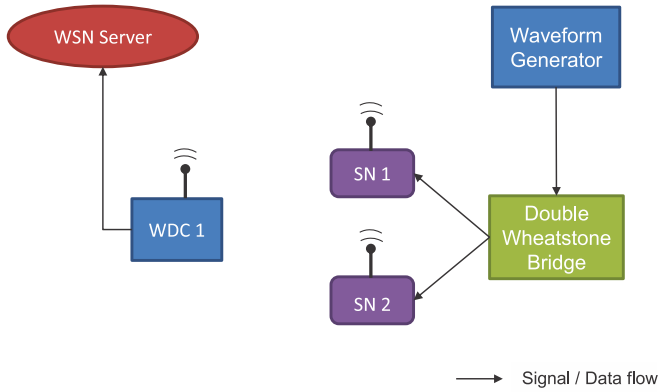

Fig. 5. Synchronization testing setup with real devices.

reliability and decouples traffic scheduling from the MAC layer by dynamically defining the slot allocation in the beacons. This is only partially done in other solutions.

B. Protocol Implementation

The protocol modes implemented for this paper correspond to four different SN operation phases, namely, configuration, sleep, data transfer, and ultra-low-power mode. Mode operation could be implemented with existing protocols by individual renegotiation of slots but that would be quite complex to use. In all four modes, a WDC broadcasts a beacon regularly. The SNs are synchronized with the beacon at a rate that depends on their operation mode. In configuration, SNs are seldom active. They are not linked to a WDC until the latter starts broadcasting association requests. During flight, they are mostly in sleep mode, with a wake-up latency of 0.5 s. In data transfer mode, a cell is performing and transferring strain measurements. SNs are active and listen to every beacon sent by their WDC. Finally, in ultra-low-power sleep, SNs and WDCs keep their association, while the aircraft is not in use, but operate at the lowest power: the WDCs are off and the SNs wake up rarely to check for WDC activity. The wake-up latency from this mode is 6 min.

Retransmissions for error recovery are also supported. Uplink traffic is acknowledged by a bit field in the beacon following transmission, as in LLDN. SNs check this field and retransmit the packet at the first opportunity. Opportunities are given in a flexible manner by the WDC, which will assign additional slots to the nodes for which it did not receive the packet. The assignment is indicated in the beacon.

C. Synchronization

A functional diagram of synchronization is shown in Fig. 4. It is assumed that the WDC is synchronized with the WSN server clock (green arrow in Fig. 4). It is also assumed that the TDMA MAC protocol operates in data transfer mode and that the SN is acquiring data. Data are kept in memory by the SN until they can be transmitted at the next slot assigned by the TDMA. The WDC provides each beacon with a beacon sequence number (BSN) and maintains a lookup table associating each BSN with the beacon transmission time (1 in Fig. 4). The SN uses its TDMA slots to transmit data samples, time-stamped with the following information: BSN, offset (time between beacon reception and first measurement) and acquisition period (2 in Fig. 4). Upon forwarding a packet to the WSN server, the WDC replaces the BSN with the corresponding time (3 in Fig. 4).

D. Evaluation

The packet arrival success rate is not expected to affect the measurement acquisition and synchronization performance in the proposed use case. This is because the data rate of the radio module (2 Mbps) and the protocol lead to an effective rate of more than 800 kbit/s, which is well above the data traffic rate required by the measurements (1 kB/s per node, corresponding to a 16-bit, 500 Hz sampling rate). In turn, this leaves room for retransmissions, which are supported by the protocol using a bitmap for negative acknowledgments.

In addition, the stationary nature of the WSN installation reduces the risk of severe dynamic disturbance at the physical layer even though the flexible retry mechanism is able to withstand links with high error rates. It is noted that for applications requiring much higher sampling rates or short latencies, the effect of packet loss should be considered, taking into account that the protocol supports retransmissions, with currently no strict maximal transmission latency requirements. On the other hand, time-stamping accuracy is essential to allow the comparison of strain measurement data with data from other systems; therefore, evaluation is focused on this aspect.

Transmission and synchronization tests were performed with two SNs and one WDC. To allow measurement of the time-stamping difference, a single signal generator was used as input to both nodes. To ensure that the SNs measure exactly the same signal on their differential input, a double Wheatstone bridge circuit was employed. The input signal is a triangle waveform. The setup is depicted in Fig. 5.

Data samples are collected by the WSN server and exported into Octave. The synchronization error is estimated by measuring the time difference between the peaks of a triangle signal acquired by the two SNs (inset of Fig. 6). Fig. 6 shows the values obtained during 1 h of acquisition. The average and maximum error are 138 and 586 μs, respectively.

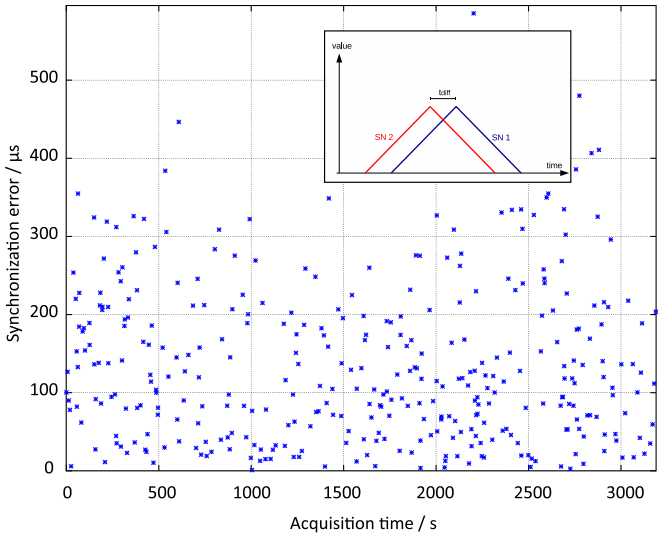

Fig. 6. Synchronization error within one cell of two nodes of Fig. 5, measured by the time difference of triangular data, as shown in the inset.

Clock deviation is not the only source of synchronization error. Implementation constraints (interrupt handling, software overhead to avoid coupling) often result in unpredictable delays between actual packet emission or reception and timestamp recording. Another source of error is timer reading during timestamp acquisition. On the processor used in the SN and WDC, this operation involves reading a running counter, which may give erroneous results. Nevertheless, the maximal difference between two measured timestamps is well below the required 1 ms for measurement synchronization. This specification would still be respected if there were more than one cells because the typical synchronization error for wired network protocols such as PTP (IEEE1588) is less than 10 μs.

Given the master−slave nature of the synchronization and the single hop topology, the same accuracy of synchronization is expected to be preserved when the number of SNs increases. However, at full network scale with up to 20 nodes per WDC, packet and WDC processing congestion, as well as transmission errors, could potentially increase the timestamp error. The high-speed data link (2 Mbps) and processing power of the WDC in comparison to the 8 kbps data acquisition rate of each SN are expected to prevent such an increase. In addition, transmission errors are mitigated by beacon redundancy and adaptive retries. Nevertheless, synchronization tests with more SNs are required for a full-scale experimental demonstration of this performance.

E. Duty Cycling and Energy Demand

The power consumption of the SN modules is presented in Table II. For the load-monitoring cases outlined in Section I, it is possible to calculate the SN energy demand during a flight. In sleep mode, the SN needs to monitor the WDC beacons two times every second, to maintain a wake-up latency below 0.5 s. Taking into account a time slot duration of 1 ms, this corresponds to a duty cycle of less than 0.2% for the MCU and RX radioactivity during sleep mode, while the rest of the SN remains at sleep.

TABLE II
POWER CONSUMPTION OF THE SN

Module	Mode	Current (mA)	Power (mW)
TI MSP430F5437A	8 MHz Active	2.5	8.25
MCU	LPM3 Sleep	0.003	0.009
Atmel AT86RF231/233	TX/RX	11.6/12.3	38.3/40.6
Radio, (at 0 dBm)	Sleep	0.0002	0.0007
SX8724S ADC with	Active	4.3	14.2
1 kΩ strain sensor	Sleep	0.00025	0.00083
Flash ST M25P80	Write/Read/Sleep	15/4/0.01	50/13/0.03
Total SN	Max/Sleep	34/0.013	113/0.04

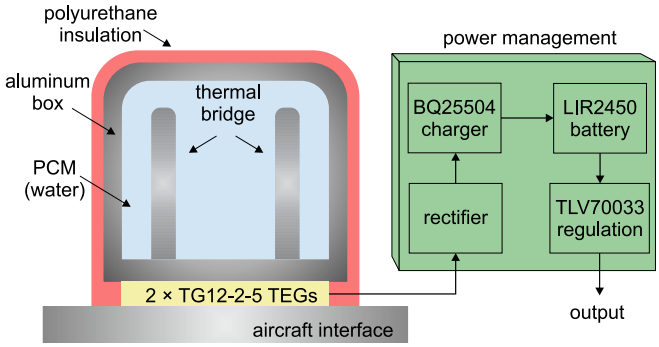

Fig. 7. Schematic of the heat storage thermoelectric power supply.

At acquisition mode, the sensing electronics are fully active, but the MCU still sleeps between its tasks, which are as follows: receive a beacon every 40 ms, transmit a data packet every 40 ms, and acquire one sample every 2 ms. This amounts to roughly 50% of activity rate for the MCU. The transceiver is active for beacon reception and packet transmission. With 1 ms slot duration and 1 ms of mode switching, the radio duty cycle is 10%.

As an application example, for a 2-hour flight and accounting for a duty-cycled measurement acquisition and transmission of 800 s, corresponding to the load monitoring cases described in Section I, the total energy demand of the SN is calculated to be 25 J, including a 20% overhead. The energy consumption that corresponds to nonacquisition SN operation is less than 1 J/h of flight. For longer flights, this can be a significant overhead; however, it can be substantially reduced by exploitation of the deep sleep mode feature of the proposed protocol.

V. POWER SUPPLY

A. Device Concept

The power supply is based on a dynamic thermoelectric harvester (see Fig. 7). An insulated heat storage unit (HSU) is used, filled with a phase change material (PCM), and in thermal contact with the environment mainly through a thermoelectric generator (TEG). The response of this system to external temperature (T_{OUT}) variation is dynamic: the HSU temperature follows T_{OUT}, with a delay determined by the in−out thermal resistance R, the HSU heat capacity C, and the latent heat L.

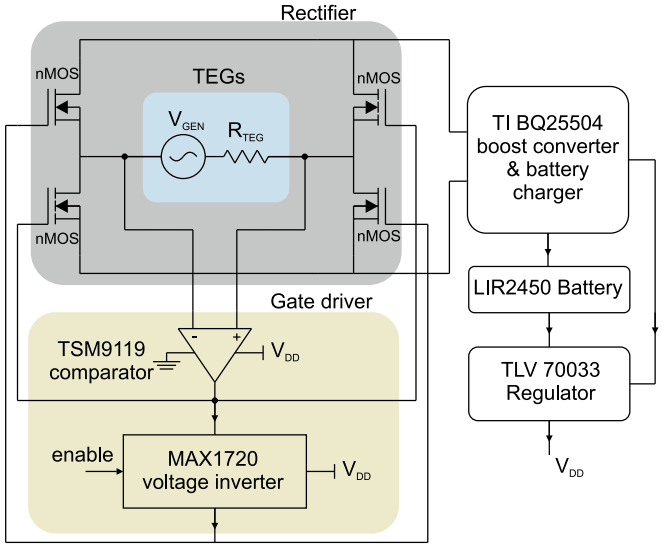

Fig. 8. Schematic of the rectifier and the power management system.

This provides a temperature difference across the TEG, and the heat flux is converted into electricity. A detailed analysis of this device concept can be found in [31]. If such a device is attached to an aircraft fuselage, during flight, T_{OUT} fluctuates from a high (ground) value to a low (cruising) value and back. Heat flows out of the HSU during takeoff and into the HSU during landing, giving a bipolar TEG output.

A schematic of the power management circuit is presented in Fig. 8. Its first stage is a custom rectifier comprising two Vishay SUD42N03 enhancement mode and two Infineon BSP149 depletion mode n-type MOSFETs with on-state resistance 3.7 mΩ and 1.7 Ω, respectively. The MOSFETs were gated by a TSM9119 comparator, using a duty-cycled MAX1720 voltage inverter for the depletion mode transistors [34]. This circuit provides a cold-starting low-voltage rectification ability, due to the normal-closed operation of the depletion MOSFETs, at the expense of additional losses due to their high on-state resistance. After rectification, the harvested power is stored in a Li-ion battery through a maximum power point tracking boost converter and battery charger chip. The power is supplied to the SN through a regulator, including battery undercharging and overcharging protection. [34].

The startup time of the power management system is below 100 ms. The cold-starting time of the power supply depends on the battery state. If the battery is at the regulator-cut-off voltage of 3.4 V, it needs to gain 80 mV before the BQ25504 chip re-enables the regulator. This is equivalent to 32.5 J for the selected battery or a 10-min takeoff of energy harvesting, as it will be shown experimentally in Section V-C. This is adequate for the sensing scenario example of this paper. Nevertheless, if desirable, the cold-starting time can be reduced by selecting a battery of lower capacity.

B. Device Fabrication

A 60 × 30 × 30 mm aluminum HSU was used, with internal fins as thermal bridges, capacity of 30 cm^3 and 2 mm

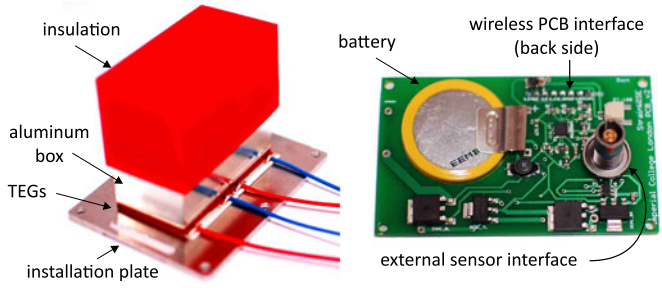

Fig. 9. Photograph of the heat storage thermoelectric generator and the power management PCB.

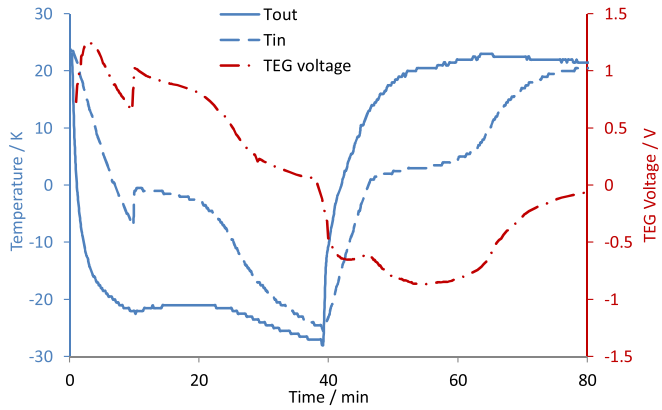

Fig. 10. Harvester temperature and voltage response to a temperature cycle corresponding to a typical flight.

polyurethane insulation. Two TG12-2-5 Marlow TEGs were employed, with ZT = 0.72, each having a thermal resistance of 3.6 K/W and an electrical resistance of 5 Ω. The HSU was filled with 23 cm^3 of distilled water. The heat storage generator and the power management PCB are shown in Fig. 9.

C. Power Supply Performance

The performance of the power supply prototypes used in the SN has been evaluated under various emulated flight test temperature conditions. Laboratory results on the generator temperature and voltage response are shown in Fig. 10. The temperature profile from +20 °C to −20 °C and back that is used corresponds to the temperature of an aircraft fuselage during a typical flight [5]. A custom 4 °C/min environmental chamber was used for the experiments. The PCM temperature was monitored by a thermocouple installed in thermal contact to the aluminum HSU. The cooldown and warm-up phase changes occur at around 10 and 45 min, respectively. During phase change, the large heat flow has a visible effect to the chamber temperature. The TEG voltage was measured in connection to the power management system.

The measured power and cumulative energy at different stages of the power management system are shown in Fig. 11. These results demonstrate 126 J of harvested energy per flight, corresponding to 5.5 J/cm^3 of PCM, or 1.62 J/cm^3 of total generator size, accounting for the total generator volume of 78 cm^3. This

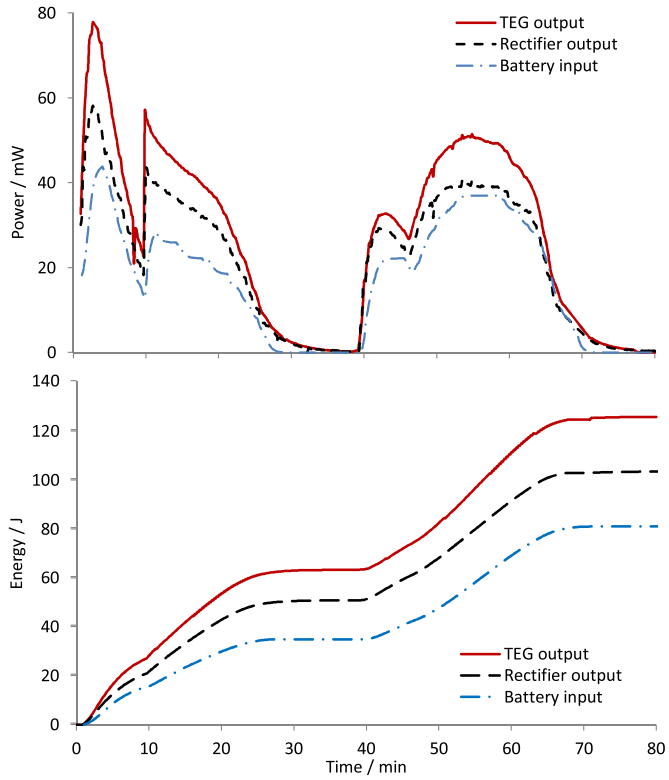

Fig. 11. Measured power (top) and cumulative energy (bottom) at different power management stages corresponding to the data of Fig. 10.

is 25% higher than 4.3 and 1.3 J/cm^3, respectively, reported for an earlier implementation [31]. This improvement can be attributed to the introduction of custom-fabricated polyurethane insulation instead of polystyrene sheets used previously and to maximum power point tracking.

The rectifier efficiency is around 70% during cooldown and 90% during warm-up. The 20% of additional loss during cooldown is due to the high resistance of the depletion MOSFETs. The remaining 10% of rectifier losses correspond to an additional 1.5 Ω series resistance of the multimeter used for current measurements. The booster efficiency was found to be 75%, demonstrating an overall TEG-to-battery efficiency of 64%, with a measured battery charge total of 79 J per flight cycle. This provides a significant allowance of operation flexibility to the SNs, which have a nominal, margin-included consumption of 25 J per flight, as detailed in Section III-B.

VI. Conclusion

The presented system is a credible and innovative response to the challenging requirements of energy-autonomous wireless strain sensing for aircrafts. It was codesigned such that the energy provided by the dynamic thermoelectric harvester during a flight is sufficient for the operation of the SNs. This was made possible by the introduction of a new harvesting prototype design with increased energy density and a new wireless communication protocol, which minimizes power consumption while ensuring responsiveness (0.5 s start-up) and a time-stamping error that is less than 1 ms. The protocol supports automatic base station discovery and ultra-low-power modes to allow functionality even after long inactivity periods.

The dynamic thermoelectric generator takes advantage of the PCM latent heat, and therefore, its phase change must lie within the temperature profile range. The aircraft skin temperature profile during typical flights ranges from above 0 °C on ground, down to around −20 °C at cruising altitudes. Hence, water, with a phase change at 0 °C, is a suitable PCM for these cases. For flights with temperature ranges that do not cross 0 °C, such as low altitude flights or flights that depart from or arrive at airports experiencing subzero temperatures, different PCMs can be used. A study of such cases can be found in [36]. The energy-autonomous WSN architecture that is introduced with this prototype system can be suited to other industrial monitoring applications.

References

[1] *Environmental Conditions and Test Procedures for Airborne Equipment*, EUROCAE – ED-14G, 2011.
[2] R. Yedavalli and R. Belapurkar, "Application of wireless sensor networks to aircraft control and health management systems," *Control Theory Technol.*, vol. 9, pp. 28–33, Feb. 2011.
[3] D. Samson, M. Kluge, T. Becker, and U. Schmid, "Energy harvesting for remote monitoring of aircraft seats," *Sensor Lett.*, vol. 8, pp. 328–335, Apr. 2010.
[4] D. C. Myhre, M. J. Buenz, J. A. Norlien, W. G. Kunik, and W. W. Williams, "Wireless tire pressure and/or wheel speed sensing system for aircraft," Patent number: 7397353, Filed: Jul. 27, 2005, Date of Patent: Jul. 8, 2008.
[5] T. Becker *et al.*, "Autonomous sensor nodes for aircraft structural health monitoring," *IEEE Sensors J.*, vol. 9, no. 11, pp. 1589–1595, Nov. 2009.
[6] A. Akl, T. Gayraud, and P. Berthou, "Investigating several wireless technologies to build a heteregeneous network for the in-flight entertainment system inside an aircraft cabin," in *Proc. 6th Int. Conf. Wireless Mobile Commun.*, Valencia, Spain, Sep. 20–25, 2010, pp. 532–537.
[7] K. Langendoen and A. Meier, "Analyzing MAC protocols for low data-rate applications," *ACM Trans. Sens. Netw.*, vol. 7, no. 1, pp. 1–34, Aug. 2010.
[8] A. El-Hoiydi and J. D. Decotignie, "WiseMAC: An ultra low power MAC protocol for the downlink of infrastructure wireless sensor networks," in *Proc. 9th Int. Symp. Comput. Commun.*, Alexandria, Egypt, Jun. 28–Jul. 01, 2004, pp. 244–251.
[9] R. Tjoa, K. L. Chee, P. K. Sivaprasad, S. V. Rao, and J. G. Lim, "Clock drift reduction for relative time slot TDMA-based sensor networks," in *Proc. IEEE 15th Int. Symp. Personal, Indoor Mobile Radio Commun.*, Barcelona, Spain, Sep. 5–8, 2004, pp. 1042–1047.
[10] S. Gobriel, D. Mosse, and R. Cleric, "TDMA-ASAP: Sensor network TDMA scheduling with adaptive slot-stealing and parallelism," in *Proc. 29th IEEE Int. Conf. Distrib. Comput. Syst.*, Montreal, QC, Canada, Jun. 22–26, 2009, pp. 458–465.
[11] X. Cao and Z. Song, "An overview of slot assignment (SA) for TDMA," in *Proc. IEEE Int. Conf. Signal Process., Commun. Comput. 2015*, Hong Kong, Sep. 19–22, 2015, pp. 1–5.
[12] A. Kanzaki, T. Hara, and S. Nishio, "On a TDMA slot assignment considering the amount of traffic in wireless sensor networks," in *Proc. Int. Conf. Adv. Inf. Netw. Appl.*, Bradford, U.K., May 26–29, 2009, pp. 984–989.
[13] L. Lin, X. Lin, and N. B. Shroff, "Low-complexity and distributed energy minimization in multihop wireless networks," in *Proc. 26th IEEE Int. Conf. Comput. Commun.*, Anchorage, AK, USA, May 6–12, 2007, pp. 1685–1693.
[14] C. Yu and E. Fleury, "A distributed policy scheduling for wireless sensor networks," in *Proc. 26th IEEE Int. Conf. Comput. Commun.*, Anchorage, AK, USA, May 6–12, 2007, pp. 1559–1567.
[15] C. Yunxia, Z. Qing, V. Krishnamurthy, and D. Djonin, "Transmission scheduling for optimizing sensor network lifetime: A stochastic shortest path approach," *IEEE Trans. Signal Process.*, vol. 55, no. 5, pp. 2294–2309, May 2007, doi 10.1109/TSP.2007.893213.
[16] G. P. Halkes and K. G. Langendoen, "Crankshaft: An energy-efficient MAC-protocol for dense wireless sensor networks," in *Wireless Sensor Networks*, vol. 4373. Berlin, Germany: Springer, pp. 228–244, Jan. 2007.

[17] *IEEE Standard for Local and Metropolitan Area Networks*, IEEE Std 802.15.4e-2012, pp. 1–225, Apr. 2012.
[18] J. Elson, L. Girod, and D. Estrin, "Fine-grained network time synchronization using reference broadcasts," in *Proc. 5th Symp. Operating Syst. Design Implement.*, Boston, MA, USA, Dec. 9–11, 2002, vol. 36, pp. 147–163.
[19] S. Ganeriwal, R. Kumar, and M. B. Srivastava, "Timing-sync protocol for sensor networks," in *Proc. 1st Int. Conf. Embedded Netw. Sensor Syst.*, Los Angeles, CA, USA, Nov. 5–7, 2003, pp. 138–149, doi: 10.1145/958491.958508.
[20] M. Maroti, B. Kusy, G. Simon, and A. Ledeczi, "The flooding time synchronization protocol," in *Proc. 2nd Int. Conf. Embedded Netw. Sensor Syst.*, Baltimore, MD, USA, Nov. 3–5, 2004, pp. 39–49.
[21] S. Nazemi Gelyan, A. Eghbali, L. Roustapoor, S. Yahyavi Firouz Abadi, and M. Dehghan, "SLTP: Scalable lightweight time synchronization protocol for wireless sensor network," in *Mobile Ad-Hoc and Sensor Networks*, vol. 4864. Berlin, Germany: Springer, pp. 536–547, Dec. 2007.
[22] M. Magno, D. Boyle, D. Brunelli, B. O'Flynn, E. Popovici, and L. Benini, "Extended wireless monitoring through intelligent hybrid energy supply," *IEEE Trans. Ind. Electron.*, vol. 61, no. 4, pp. 1871–1881, Apr. 2014.
[23] S. Moss, A. Barry, I. Powlesland, S. Galea, and G. P. Carman, "A low profile vibro-impacting energy harvester with symmetrical stops," *Appl. Phys. Lett.*, vol. 97, Dec. 2010, Art. no. 234101.
[24] S. W. Arms *et al.*, "Energy harvesting wireless sensors and networked timing synchronization for aircraft structural health monitoring," in *Proc. 1st Int. Conf. Wireless Commun., Veh. Technol., Inf. Theory Aerosp. Electron. Syst. Technol.*, Aalborg, Denmark, pp. 16–20, May 17–20, 2009.
[25] S. R. Anton, A. Erturk, and D. J. Inman, "Energy harvesting from small unmanned air vehicles," in *Proc. 17th Int. Symp. Appl. Ferroelectr., 3rd Annu. Energy Harvesting Workshop*, Santa Fe, NM, USA, Feb. 23–28, 2008, pp. 145–146.
[26] K. C. Magoteaux, B. Sanders, and H. A. Sodano, "Investigation of an energy harvesting small unmanned air vehicle," *SPIE Proc., Active Passive Smart Struct. Integr. Syst.*, vol. 6928, pp. 92823–92823, Apr. 18, 2008.
[27] D. Zhu, S. P. Beeby, M. J. Tudor, and N. R. Harris, "A credit card sized self powered smart sensor node," *Sens. Actuators. A*, vol. 169, no. 2, pp. 317–325, Oct. 2011.
[28] S. Lee and B. D. Youn, "A new piezoelectric energy harvesting design concept: Multimodal energy harvesting skin," *IEEE Trans. Ultrason., Ferroelectr., Freq. Control*, vol. 58, no. 3, pp. 629–645, Mar. 2011.
[29] K. D. Song, T. B. Stout, S. Yang, J. Kim, and S. H. Choi, "Energy harvesting of dipole rectenna for airship applications," *SPIE Proc., Nanosens., Microsens., Biosens. Syst.*, vol. 6528, pp. U135–U144, Apr. 2007.
[30] G. Liu, N. Mrad, G. Xiao, Z. Li, and D. Ban, "RF-based power transmission for wireless sensors nodes," in *Proc. Smart Mater., Struct. NDT Aerospace*, Montreal, QC, Canada, Nov. 2–4, 2011, pp. 2–4.
[31] M. E. Kiziroglou, S. W. Wright, T. T. Toh, P. D. Mitcheson, T. Becker, and E. M. Yeatman, "Design and fabrication of heat storage thermoelectric harvesting devices," *IEEE Trans. Ind. Electron.*, vol. 61, no. 1, pp. 302–309, Jan. 2014.
[32] D. Samson, T. Otterpohl, M. Kluge, U. Schmid, and T. Becker, "Aircraft-specific thermoelectric generator module," *J. Electron. Mater.*, vol. 39, pp. 2092–2095, Sep. 2010.
[33] N. Marchenko, T. Andre, G. Brandner, W. Masood, and C. Bettstetter, "An experimental study of selective cooperative relaying in industrial wireless sensor networks," *IEEE Trans. Ind. Electron.*, vol. 10, no. 3, pp. 1806–1816, Aug. 2014.
[34] T. T. Toh, S. W. Wright, M. E. Kiziroglou, P. D. Mitcheson, and E. M. Yeatman, "A dual polarity, cold-starting interface circuit for heat storage energy harvesters," *Sens. Actuators A*, vol. 211, pp. 38–44, May 2014.
[35] Sony Corp., *CR 2032 Lithium manganese dioxide battery specs* [Online]. Available: http://www.sony.net/Products/MicroBattery/cr/spec.html, accessed 2016.
[36] A. Elefsiniotis *et al.*, "Performance evaluation of a thermoelectric energy harvesting device using various PCMs," in *Proc. 13th Power MEMS, J. Phys., Conf. Ser. 476 012020*, London, U.K., Dec. 3–6, 2013, doi: 10.1088/1742-6596/476/1/012020.

Authors' photographs and biographies not available at the time of publication.